

Report of Investigations 2002-1

**Tsunami hazard maps of the  
Kodiak area, Alaska**

by

E.N. Suleimani, R.A. Hansen, R.A. Combellick, G.A. Carver,  
R.A. Kamphaus, J.C. Newman, and A.J. Venturato



**Published by**

STATE OF ALASKA

DEPARTMENT OF NATURAL RESOURCES

DIVISION OF GEOLOGICAL & GEOPHYSICAL SURVEYS

**2002**



# Report of Investigations 2002-1

## TSUNAMI HAZARD MAPS OF THE KODIAK AREA, ALASKA

by  
E.N. Suleimani, R.A. Hansen, R.A. Combellick, G.A. Carver,  
R.A. Kamphaus, J.C. Newman, and A.J. Venturato

2002

This is a joint publication of the Alaska Division of Geological & Geophysical Surveys and the Geophysical Institute, University of Alaska Fairbanks, in cooperation with the Kodiak Island Borough and the City of Kodiak.

Maps and text may be purchased separately. Maps are \$13.00 each; text is \$2.00.



Kodiak Island Borough



City of Kodiak

This DGGGS Report of Investigations is a final report of scientific research. It has received technical review and may be cited as an agency publication.



STATE OF ALASKA  
Tony Knowles, *Governor*

DEPARTMENT OF NATURAL RESOURCES  
John T. Shively, *Commissioner*

DIVISION OF GEOLOGICAL & GEOPHYSICAL SURVEYS  
Milton A. Wiltse, *Director and State Geologist*

Division of Geological & Geophysical Surveys publications can be inspected at the following locations. Address mail orders to the Fairbanks office.

Alaska Division of Geological  
& Geophysical Surveys  
794 University Avenue, Suite 200  
Fairbanks, Alaska 99709-3645

University of Alaska Anchorage Library  
3211 Providence Drive  
Anchorage, Alaska 99508

Elmer E. Rasmuson Library  
University of Alaska Fairbanks  
Fairbanks, Alaska 99775-1005

Alaska Resource Library  
3150 C Street, Suite 100  
Anchorage, Alaska 99503

Alaska State Library  
State Office Building, 8th Floor  
333 Willoughby Avenue  
Juneau, Alaska 99811-0571

This publication released by the Division of Geological & Geophysical Surveys was produced and printed in Fairbanks, Alaska at a cost of \$54 per copy. Publication is required by Alaska Statute 41, "to determine the potential of Alaskan land for production of metals, minerals, fuels, and geothermal resources; the location and supplies of groundwater and construction materials; the potential geologic hazards to buildings, roads, bridges, and other installations and structures; and shall conduct such other surveys and investigations as will advance knowledge of the geology of Alaska."

# CONTENTS

Abstract .....	1
Introduction .....	1
Kodiak Island region .....	2
Numerical model grids .....	3
Grid development .....	4
Data sources .....	4
Grid products .....	4
Source model for the 1964 tsunami .....	5
Modeling of the 1964 tsunami in Kodiak .....	6
Hypothetical tsunami scenarios .....	7
Inundation modeling results .....	11
Local observations .....	11
Time histories .....	12
Sources of error .....	12
Summary .....	15
Acknowledgments .....	16
References cited .....	16

## FIGURES

Figure 1. Map of the Gulf of Alaska with major faults and rupture zones of the 1938, 1946, and 1964 earthquakes .....	2
2. Photo showing damage in downtown Kodiak resulting from the tsunami of March 27, 1964.....	3
3. Map of Kodiak Island grid of 24-arc-second resolution .....	3
4. Map of slip distribution of the 1964 earthquake, from Johnson and others (1996).....	6
5. Map of surface deformation of the 1964 earthquake .....	7
6. Maps of observed and computed inundation lines for the Kodiak downtown area and USCGR.....	8
7. Map of rupture area of the 1964 earthquake modeled as a single fault .....	9
8. Map of rupture areas of the two hypothetical earthquakes in the Alaska–Aleutian megathrust zone .....	10
9. Map of rupture area of Narrow Cape fault divided into three subfaults .....	10
10. Map of hypothetical event in the Cascadia subduction zone modeled as a single fault .....	11
11. Graph of time histories of modeled tsunami waves at Kodiak city harbor.....	13
12. Graph of time histories of the modeled tsunami waves at Shahavka Cove .....	13
13. Graph of time histories of the modeled tsunami waves offshore the mouth of Buskin River .....	14
14. Graph of velocity time histories in Near Island channel and at the mouth of Buskin River .....	14

## TABLES

Table 1. Data sources used for grid development .....	5
2. Delivered grid summary.....	5
3. Fault rupture parameters for single-fault scenarios.....	8
4. Slip distribution for the Narrow Cape scenarios .....	11
5. Some critical parameters at 9 locations indicated on sheets 3 and 4 .....	12

## SHEETS

[in envelope]

Sheet 1. Tsunami inundation scenarios for the Kodiak area, Alaska: city of Kodiak and vicinity	
2. Tsunami inundation scenarios for the Kodiak area, Alaska: Womens Bay and U.S. Coast Guard Reservation	
3. Tsunami hazard maps of the Kodiak area, Alaska: city of Kodiak and vicinity	
4. Tsunami hazard maps of the Kodiak area, Alaska: Womens Bay and U.S. Coast Guard Reservation	



# TSUNAMI HAZARD MAPS OF THE KODIAK AREA, ALASKA

by

E.N. Suleimani<sup>1</sup>, R.A. Hansen<sup>1</sup>, R.A. Combellick<sup>2</sup>, G.A. Carver<sup>3</sup>,  
R.A. Kamphaus<sup>4</sup>, J.C. Newman<sup>4</sup>, and A.J. Venturato<sup>4</sup>

## Abstract

This report is intended to provide guidance to local emergency managers in tsunami hazard assessment. Tsunami waves are a real threat for many Alaskan coastal locations, and community preparedness plays an important role in saving lives and property in a case of such a disaster. In this work we used a numerical modeling method to study tsunami waves generated by earthquake sources. We considered several hypothetical tsunami scenarios with a potential to generate tsunami waves that can affect communities in the Kodiak vicinity. Our results confirm that among the earthquake-generated tsunamis we modeled, the 1964 event can be considered a worst-case scenario for future planning. Although our tsunami models included a local fault source, we did not model local landslide-generated waves. Results of numerical modeling combined with historical observations can be very helpful in evacuation planning and public education for reducing risks from future tsunamis.

## INTRODUCTION

Alaska has the greatest earthquake and tsunami potential in the entire United States. Kodiak Island lies in one of the most seismically active regions of Alaska, where the Pacific Plate is subducting under the North American Plate (fig. 1). This subduction zone, the Alaska–Aleutian megathrust zone, creates high tsunami hazards for the adjacent coastal areas. The coseismic crustal movements that characterize this area have a high potential for producing vertical sea floor displacements, which are highly tsunamigenic. Historic tsunamis that were generated by earthquakes in the Alaska–Aleutian subduction zone have resulted in widespread damage and loss of life along the Alaskan Pacific coast and other exposed locations around the Pacific Ocean. Large seismic events occurring in the vicinity of the Alaska Peninsula, Aleutian Islands, and Gulf of Alaska have a very high potential for generating both local and Pacific-wide tsunamis. Seismic water waves originating in Alaska can travel across the Pacific and destroy coastal towns hours after they are generated. However, they are considered to be a near-field hazard for Alaska, and can reach Alaskan coastal communities within minutes after the earthquake. Therefore, saving lives and property depends on how well a community is prepared, which makes it essential to estimate the potential flooding area of the coastal zones in a case of a local or distant tsunami.

To help mitigate the risk these earthquakes and tsunamis pose to Alaskan coastal communities, the Geophysical Institute (GI) of the University of Alaska Fairbanks and the State of Alaska, Department of Natural Resources, Division of Geological & Geophysical Surveys (ADGGS) participate in the National Tsunami Hazard Mitigation Program (NTHMP) by evaluating and mapping potential inundation of selected parts of Alaska coastlines using numerical modeling of tsunami wave dynamics. The communities for inundation modeling are selected in coordination with the Alaska Division of Emergency Services (ADES) with consideration to location, infrastructure, availability of bathymetric and topographic data, and willingness for a community to incorporate the results in a comprehensive mitigation plan.

Kodiak Island was identified as a high-priority region for Alaska inundation mapping. It has a number of communities with relatively large populations and significant commercial resources. The preferred sites for runup modeling were determined by ADES and Kodiak local government officials to be the three communities of metropolitan Kodiak: Kodiak city, U.S. Coast Guard Reservation (USCGR) and Womens Bay. Emergency managers need tsunami evacuation maps for these communities, showing the extent of inundation with respect to human and cultural features, and evacuation routes.

<sup>1</sup>Alaska Earthquake Information Center, Geophysical Institute, University of Alaska, P.O. Box 757320, Fairbanks, Alaska 99775-7320.

<sup>2</sup>Alaska Division of Geological & Geophysical Surveys, 794 University Avenue, Suite 200, Fairbanks, Alaska 99709-3645.

<sup>3</sup>Humboldt State University, P.O. Box 52, Kodiak, AK 99615.

<sup>4</sup>Pacific Marine Environmental Laboratory, National Oceanic & Atmospheric Administration, 7600 Sand Point Way NE, Seattle, Washington 98125.

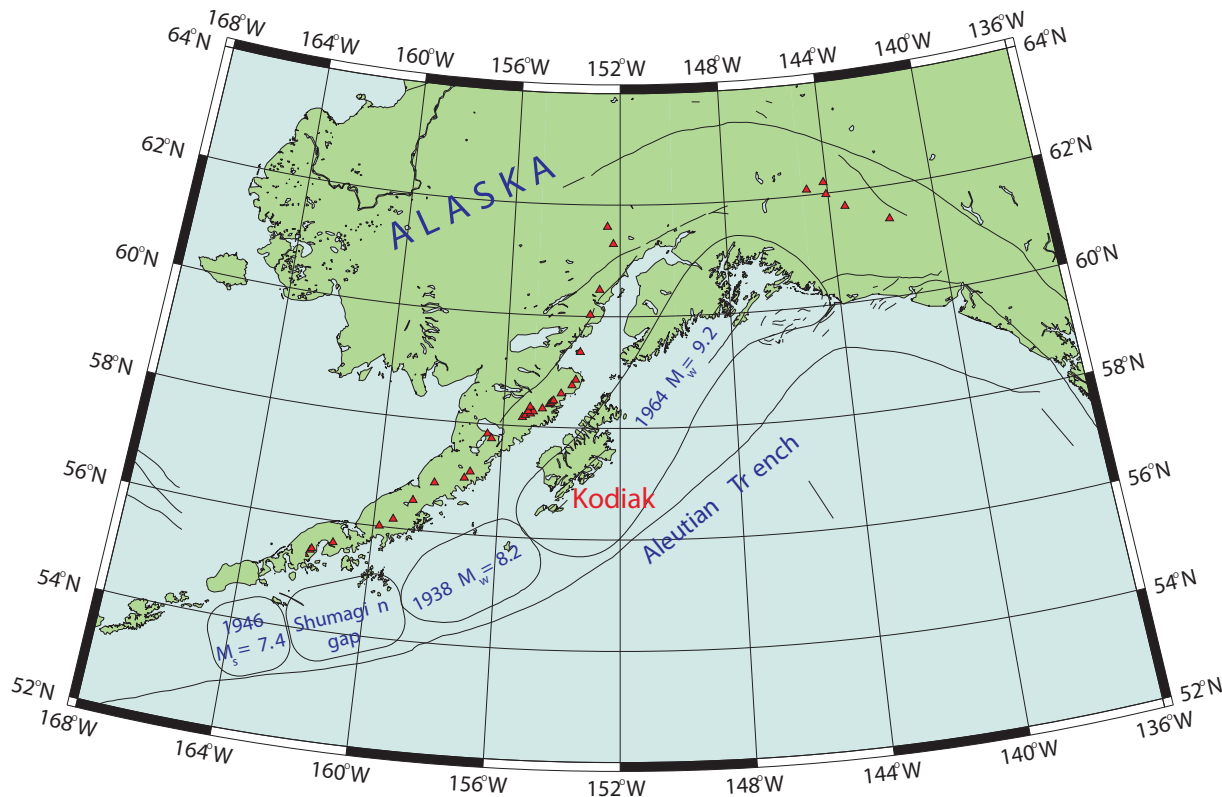


Figure 1. Map of the Gulf of Alaska with major faults and rupture zones of the 1938, 1946, and 1964 earthquakes. Red triangles indicate active volcanoes.

The production of tsunami evacuation maps consists of several stages. First, hypothetical tsunami scenarios are constructed based on the parameters of potential underwater earthquakes. Then, model simulations are performed for each of the earthquake source scenarios. The results are compared with any observations from historical tsunamis in the region, if such data exist. Finally, numerical results and historical observations are combined in order to develop a worst case scenario for a tectonically generated tsunami for every community on a map. The inundation line produced by this scenario becomes a basis for local tsunami hazard planning and construction of evacuation maps. Our analysis did not include waves produced from submarine landslides.

The tsunami hazard maps of the Kodiak area described in this report represent the first step in the State of Alaska tsunami hazard evaluation and production of inundation maps for many Alaskan coastal communities. The inundation lines calculated for seven different tsunami scenarios are shown in sheet 1 for the city of Kodiak and in sheet 2 for USCGR and Womens Bay. Sheets 3 and 4 show the extent of inundation in the same communities resulting from the “worst case scenario,” which is the maximum inundation of all modeled scenarios as well as areas of observed 1964 tsunami effects that extended farther inland than all of the modeled inundations. On the

basis of local knowledge of detailed topography, we made adjustments to the “worst case scenario” inundation lines of sheets 3 and 4. These adjustments are discussed in the “Sources of error” section.

## KODIAK ISLAND REGION

Kodiak Island is the largest island in Alaska and second largest in the United States after Hawaii. It is a region rich in fish and the location of some of the most fertile salmon streams in the world. Kodiak is one of the state’s largest fishing ports, home to nearly 800 commercial fishing vessels and large seafood processing facilities located on the waterfront and exposed to potential tsunami effects. The largest U.S. Coast Guard Reservation in the nation is located on Kodiak Island and is also sited on low-lying areas potentially at risk from locally generated tsunamis. The city of Kodiak plays an important role in regional transportation by serving southwestern Alaska communities with consumer goods. The population of the island is about 15,000 people. Kodiak’s vulnerability to tsunamis was demonstrated by the 27 March 1964 earthquake (moment magnitude 9.2). In Kodiak city, the tsunami caused six fatalities and about \$30 million in damage (fig. 2). Since then, the harbor and waterfront area of the city that was destroyed by the 1964 tsunami has

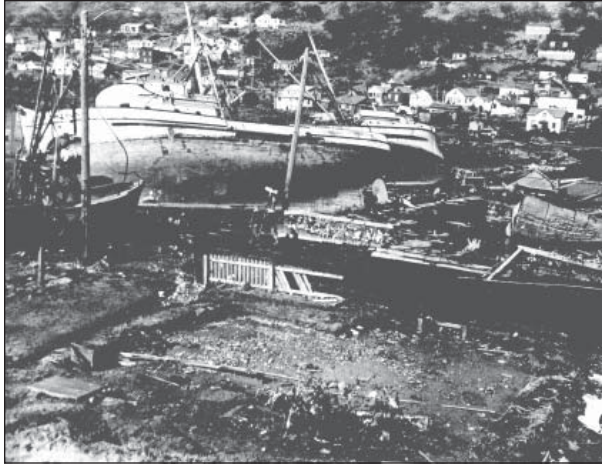


Figure 2. Damage in downtown Kodiak resulting from the tsunami of March 27, 1964, in a view looking west from the intersection of Marine Way and Mill Bay Road (see fig. 6 for location). Visible in this photograph are boats swept from the harbor and foundations of structures destroyed by the tsunami waves. Photo by U.S. Navy, March 28, 1964 (from Kachadoorian and Plafker, 1967).

been rebuilt and significantly expanded, and substantial additional growth of the city of Kodiak and other nearby communities has occurred.

In March of 1998, site visits and exploratory meetings were conducted on Kodiak Island for the purpose of evaluating Kodiak regional needs for tsunami inundation maps. This activity was a component of the NTHMP that is intended to provide assistance to coastal communities with tsunami hazard assessment. As a result, the three communities of Kodiak city, USCGR, and Womens Bay were selected for inundation modeling out of six Kodiak Island communities that were of immediate concern.

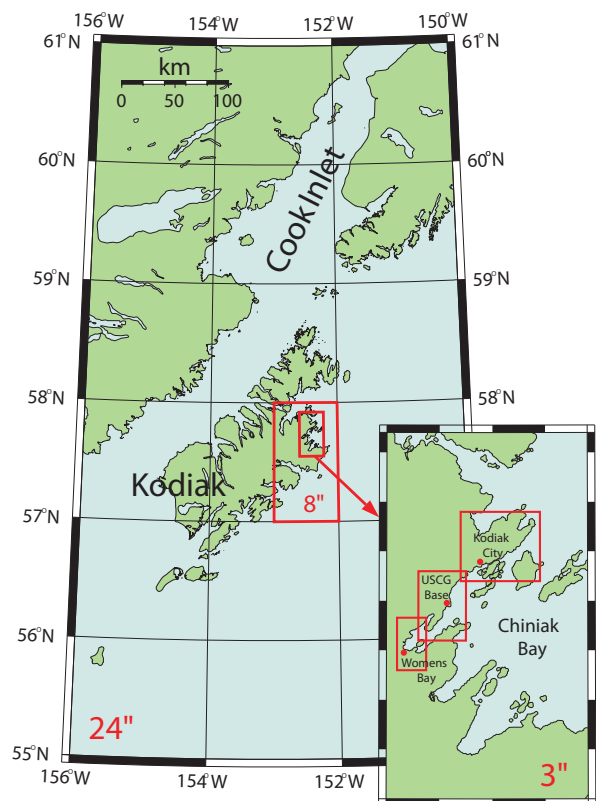
## NUMERICAL MODEL AND GRIDS

We calculated the extent of inundation caused by tsunami waves using numerical modeling of tsunami wave runup. The model is based on the vertically integrated nonlinear shallow water equations of motion and continuity with friction and Coriolis force (Murty, 1984). We applied a space-staggered grid, which require either sea level or velocity as a boundary condition. The first order scheme was applied in time and the second order scheme was applied in space. Integration was performed along the north–south and west–east directions separately as described by Kowalik and Murty (1993a).

Figure 3. Kodiak Island grid of 24-arc-second resolution. The two rectangles delineate the 8-second and the 3-second grids. Inset figure shows the 3-second grid, which includes finer resolution grids for the Kodiak Island communities of Kodiak city, USCGR and Womens Bay, where runup calculations were performed.

In order to propagate the wave from a source to various coastal locations we used embedded grids, placing a coarse grid in deep water and coupling it with finer grids in shallow water areas. We used an interactive grid splicing, therefore the equations were solved on all grids at each time step, and the values along the grid boundaries were interpolated at the end of every time step (Troshina, 1996). The radiation condition was applied at the open (ocean) boundaries (Reid and Bodine, 1968). At the water–land boundary, the moving boundary condition was used in those grids that cover areas selected for inundation mapping (Kowalik and Murty, 1993a). In all other grids, the velocity component normal to the coastline was assumed to be zero.

The region shown in figure 1 is covered by the largest grid of 2-arc-minute resolution. We used four embedded grids in order to increase resolution from 2 arc minutes (2 km x 3.7 km at 55°N latitude) in the Gulf of Alaska to 1 arc second (21.8m x 27.5m at 57°47' latitude) in the three grids that cover communities selected for inundation modeling. The embedded grids are shown in figure 3. The first grid of 24-second resolution covers the lower part of Cook Inlet and waters around Kodiak Island. The 8-second grid covers the northeast segment of the island, and the 3-second grid covers Chiniak Bay. Three more fine resolution (1 second) grids cover regions of Kodiak Island where runup calculations were performed. They are shown as three rectangles in the Chiniak Bay grid. In



these grids, the combined bathymetric and topographic data allowed for application of the moving boundary condition as well as calculating the runup heights and extent of the inundation.

There are several limitations of the model. It does not take into account the periodical change of sea level due to tides. We conducted all model runs using bathymetric data that correspond to Mean Higher High Water (MHHW). As for the generation mechanism, we modeled only earthquakes as potential sources of tsunami waves. In 1964, there were about 20 local submarine and subaerial landslide-generated waves that were limited to the bays of generation and caused substantial damage. Landslide wave sources were not considered within the scope of this generation model.

## GRID DEVELOPMENT

The Center for Tsunami Inundation Mapping Efforts (TIME), National Oceanic & Atmospheric Administration, created six data grids for the Kodiak region using the best available bathymetry and topography. TIME developed data grids using the following five-step process of (1) data collection, (2) data assessment, (3) grid computation, (4) grid assessment, and (5) product delivery. The best available bathymetric and topographic data were obtained from government and private industries. These data were converted into a usable format and then analyzed for quality using Generic Mapping Tools (GMT) software. Data sets were first converted into a latitude, longitude, and depth (xyz) format. Each data set was converted to the horizontal datum of North American Datum of 1927. Bathymetric data were converted from a vertical datum of Mean Lower Low Water to Mean Higher High Water. Topographic data were converted from a vertical datum of Mean Sea Level to Mean Higher High Water.<sup>5</sup> The vertical datum conversion was based on tidal data obtained over a 5-year period (1994–1998) from the Kodiak Island National Ocean Service water level station (station number 945-7292). The mean values were calculated by National Ocean Service using the 1960–1978 tidal epoch and were assumed constant throughout the Chiniak Bay region.

A combined bathymetric and topographic data grid was then generated using GMT. Script programming was used to compile the various data sets into a single data set and then an interpolation algorithm was applied to generate the grid. The computed grid was analyzed for quality.

Comparisons were made between the original data sets and the grid. Datums were verified and point blunders were removed. Lower resolution grids were clipped to contain only bathymetric data. Null data points were assigned a value of 9999. This procedure was repeated for each requested grid.

The grids were sent electronically to the Geophysical Institute (GI), University of Alaska Fairbanks, along with a short summary and images detailing source density and grid coverage. GI reviewed each grid and TIME made minor modifications on the basis of requests from the modeler.

## DATA SOURCES

The data sources for the grids are described in table 1. The resolution of each data source varied from approximately 10–200 meters. Many sources were in different formats, which may lead to a small conversion error. The vertical accuracy of the data is based on the root mean square error, which results in approximately 5 percent of depth for bathymetry and one-half of the contour interval for topography.

## GRID PRODUCTS

TIME delivered six grids to GI. Each grid is described in table 2. All grids were delivered in xyz format and had the following parameters:

- Grid Generation Software: Generic Mapping Tools, Version 3.3.1
- Grid Algorithm: surface interpolation method for all except Womens Bay, for which we used triangulation<sup>6</sup>
- Horizontal Datum: North American Datum of 1927
- Vertical Datum: Mean Higher High Water<sup>7</sup>
- Projection: Geographic
- Units: decimal degrees to the sixth decimal place
- Z Units: meters
- Null values: 9999

The accuracy of the final grids is based on the level of detail of the source and the grid interval used to sample the source. The topographic data set derived from the USGS DEMs has standard maximum vertical error of 10 m, which is one-half the contour interval.

<sup>5</sup>The topographic source data has a vertical datum of National Geodetic Vertical Datum of 1929 (NGVD29). However, there is no direct correlation between NGVD29 and Mean Higher High Water in this region. Therefore, Mean Sea Level was used as an estimate for NGVD29 to correct the topography to Mean Higher High Water. This is a valid approximation since NGVD29 is defined by observed height of mean sea level at 26 tide stations across the United States and Canada.

<sup>6</sup>Triangulation method was used in the Womens Bay area due to unacceptable errors produced by surface interpolation. Limited bathymetry and topography in this region may explain the problems encountered with the surface algorithm. Triangulation produced a more accurate depiction of the actual elevations in the area.

<sup>7</sup>Tidal conversion was only applied to the 1-arcsecond and 3-arcsecond high-resolution grids.

## SOURCE MODEL FOR THE 1964 TSUNAMI

We initiated this project with the modeling of the Alaska 1964 tsunami, because this event is probably the worst-case scenario of a tsunami for the Kodiak Island communities and is useful for testing the results of our modeling on the basis of a well documented historical event. The 1964 Prince William Sound earthquake generated one of the most destructive tsunamis observed in Alaska and the west coast of the U.S. and Canada. This major tectonic tsunami was generated in the trench and upper plate fold and thrust belt area of the subduction zone (Plafker and others, 2000) and affected all the communities in Kodiak and the nearby islands. On Kodiak the 1964 tsunami was studied in depth by several investigators (e.g. Kachadoorian and Plafker, 1967; Wilson and

Torum, 1968), and their observed inundation patterns are available for calibration of the model. We used output of a submarine seismic source model as an initial condition for ocean surface displacement that then propagates away from the source. The amplitude of this initial disturbance is one of the major factors that affect the resulting runup amplitudes along the shoreline. Here we used an algorithm developed by Okada (1985) to calculate the distribution of coseismic uplift and subsidence resulting from the motion of the buried fault. The fault parameters that are required to compute the deformation of the ocean bottom are location of the epicenter, area of the fault, dip, rake, strike, and amount of slip on the fault. However, the rupture area of the 1964 earthquake was too large to be adequately described by a simple one-fault model. It was demonstrated by Christensen and Beck (1994) that there were two areas of high moment release, representing the

Table 1. *Data sources used for grid development*

Media Source	Media	Data	Description
National Geodetic Data Center (NGDC)	CD-ROM (GEODAS Version 3.3)	National Ocean Service (NOS) hydrographic surveys	Bathymetric data collected 1932–2000
NGDC	CD-ROM (GEODAS Version 4.0)	Marine Trackline Geophysics	Bathymetric data from ship tracklines obtained 1850–2000
Scientific Fisheries System Incorporated (SciFish)	Electronic xyz file	NGDC bathymetric and NOS shoreline data	Bathymetric data obtained from NGDC/NOS and combined by SciFish
Alaska Geospatial Data Clearinghouse	Digital Elevation Models	USGS topographic data	10 m and 1-, 2-, and 3-arcsecond topographic data
U.S. Army Corps of Engineers (USACE)	Electronic xyz files	USACE hydrographic surveys	Bathymetric data collected in 2000

Table 2. *Delivered grid summary*

Region	Name	Resolution	Extents	Delivery Date
Kodiak and Cook Inlet	new2kod24sec	24 arc seconds	SW: -156.000000, 55.000000 NE: -150.000000, 62.000000	05/22/2000
Northeast Kodiak	newKod8sec	8 arc seconds	SW: -153.000000, 57.000000 NE: -152.000000, 58.000000	09/14/1999
Chiniak Bay	ki_3secgrid	3 arc seconds	SW: -152.600000, 57.586667 NE: -152.266667, 57.926667	01/25/2001
Kodiak City	kc1.3x0.8sec	1.3x0.8 arc seconds	SW: -152.458519, 57.766667 NE: -152.308148, 57.841481	12/07/2000
USCG Reservation	uscg1.3x0.8sec	1.3x0.8 arc seconds	SW: -152.533333, 57.708148 NE: -152.450370, 57.779259	12/07/2000
Womens Bay	wb1.3x0.8sec	1.3x0.8 arc seconds	SW: -152.622222, 57.729630 NE: -152.533333, 57.708148	12/07/2000

two major asperities of the 1964 rupture zone: the Prince William Sound asperity and the Kodiak Island asperity. A detailed analysis of the 1964 rupture zone was presented by Johnson and others (1996) through joint inversion of the tsunami waveforms and geodetic data. These authors derived a detailed slip distribution for the 1964 earthquake, which is shown in figure 4.

To construct a source function for the 1964 event, we used the fault dislocation model developed by Johnson and others (1996) that has eight subfaults representing the Kodiak asperity, and nine subfaults in the Prince William Sound asperity. The authors didn't include the Patton Bay fault on Montague Island in the source mosaic, because the contribution of this fault to the tsunami waveforms was negligible. However, they removed the effect of this fault by subtracting the deformation due to the fault from all geodetic observations. We used the equations of Okada (1985) to calculate the distribution of coseismic uplift and subsidence resulting from the given slip distribution (fig. 5). Then, the derived surface deformation was used as the initial condition for tsunami propagation. During a model run, the initial topography was modified to account for residual seismic deformation of land due to an earthquake.

## MODELING OF THE 1964 TSUNAMI IN KODIAK

We modeled the 1964 tsunami wave using two different source functions. The first one, described above, consists of 17 subfaults, each having its own parameters (scenario 1 on sheets 1 and 2). The second source function represents a single fault with uniform slip distribution (scenario 2). The amount of slip on the single fault was calculated in a way that preserves the seismic moment corresponding to the moment magnitude of 9.2. We assume that the initial displacement of the ocean surface from the equilibrium position is equal to vertical displacement of the ocean floor due to the earthquake rupture process. The model doesn't take into account the propagation of the moving rupture along the fault. We assume here that the bottom movement was instantaneous. Then, the model propagates this initial displacement from the source to coastal locations through the set of embedded grids of increasing resolution. For the communities of Kodiak city and the Kodiak Naval Station the observed inundation was documented in July of 1964 by Kachadoorian and Plafker (1967). Kodiak city, the largest community on the island, suffered the greatest damage from the tsunami.

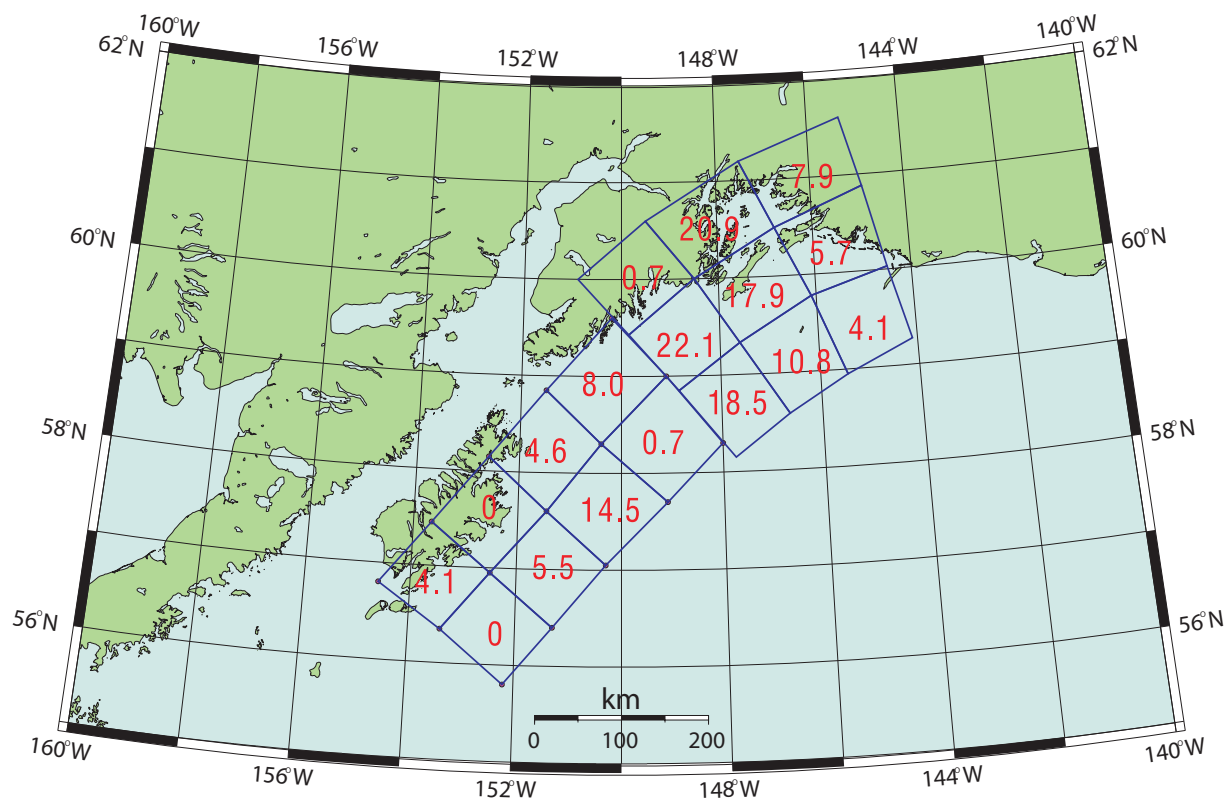


Figure 4. Slip distribution of the 1964 earthquake, from Johnson and others (1996). Numbers represent slip in meters on each subfault.

Figure 6 shows computed and observed inundation lines for the city of Kodiak and USCGR (formerly the Kodiak Naval Station). The blue line delineates the area inundated in 1964 following data collected after the event by the U.S. Army Corps of Engineers, U.S. Navy, and other authorities. The solid red line shows the inundated area computed using the complex source function of 17 subfaults. The dashed red line is for the computed inundation zone that corresponds to the simple one-fault source model. The observed area of maximum inundation at the Kodiak Naval Station is taken from Kachadoorian and Plafker (1967). The results show that the wave generated by the complex source model with detailed slip distribution produces the inundation zone closest to that observed in 1964. The one-fault model greatly underestimates the extent of flooding caused by the 1964 tsunami wave.

### HYPOTHETICAL TSUNAMI SCENARIOS

We considered several hypothetical earthquake scenarios as potential sources of tsunami waves that can affect the Kodiak Island communities. These scenarios represent both distant and local sources, and we model them using

a simple one-fault source function as well as the multiple fault approach. There are seven different tsunami inundation limits on sheets 1 and 2 that correspond to seven different tsunami scenarios. Here they are described in the order they appear on the map legend.

**Scenario 1. Repeat of 1964 event: 17 subfaults.** This source model is described in detail in the above section, “The source model for the 1964 tsunami.”

**Scenario 2. Modified 1964 event: One fault with uniform slip.** Our goal here was to provide a comparison with scenario 1 to show the importance of the detailed slip distribution of the rupture zone for the near-field inundation modeling and hazard assessment. To accomplish that, we constructed another source function for the 1964 event, consisting of a single fault with uniform slip distribution. The amount of slip on the single fault was calculated in a way that preserves the seismic moment. The resulting surface deformation was computed using the Okada (1985) algorithm and used in the tsunami model as an initial condition. The approximate fault rupture

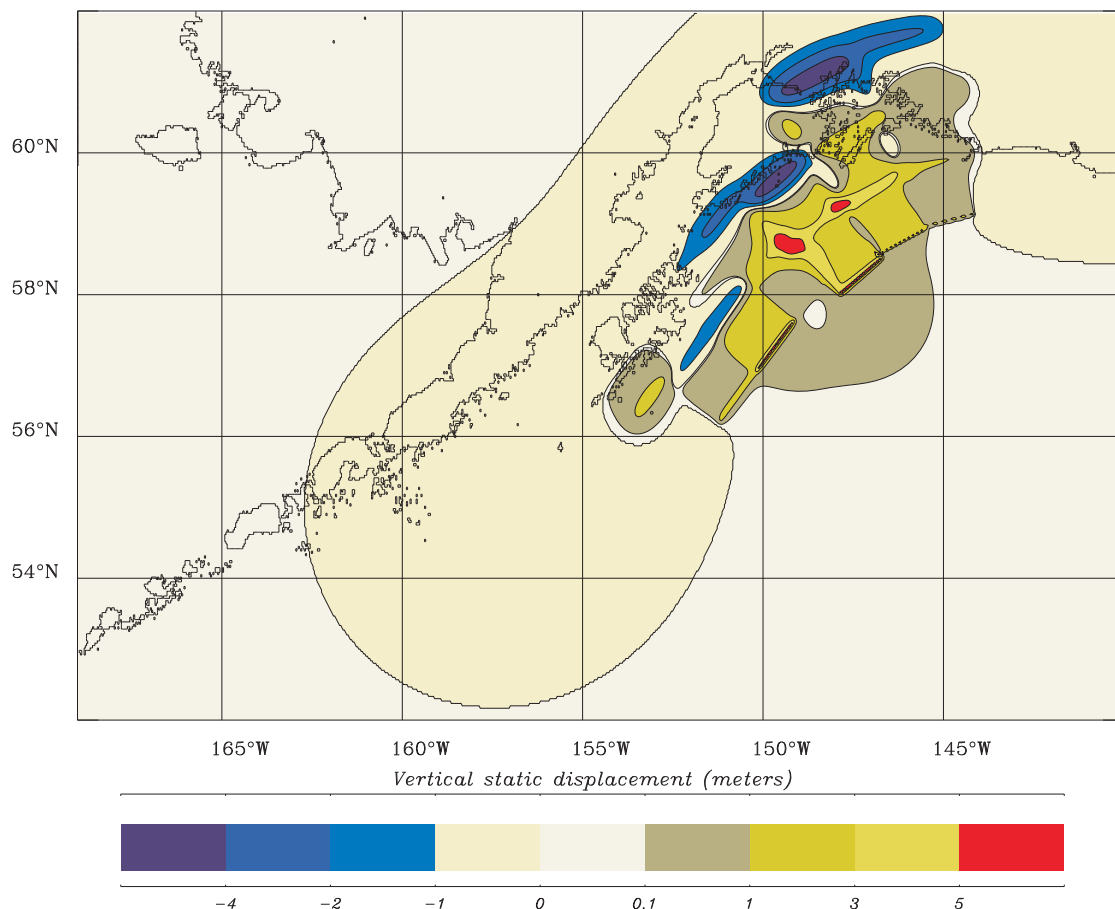


Figure 5. Surface deformation of the 1964 earthquake, calculated from the slip distribution given in figure 4.

area is shown in figure 7. Table 3 summarizes the main parameters of the single-fault scenarios.

**Scenario 3. Modified 1964 event: Kodiak asperity only, eight subfaults.** This source function represents the lower (southern) asperity of the 1964 rupture zone. According to Christensen and Beck (1994), the two segments of this zone behaved independently in the past, with the Kodiak Island region rupturing more frequently. That allowed us to consider the Kodiak asperity of the 1964 rupture as an independent source with a potential of generating tsunami waves. We modeled this source using the eight most southwestern subfaults of the 1964 fault mosaic as shown in figure 4.

**Scenario 4. Modified 1964 event: Kodiak asperity only, uniform slip.** This scenario describes the same hypothetical event as scenario 3, but with uniform slip distribution within the rupture area, which is shown in figure 8. Scenarios 3 and 4 have the same seismic moment.

**Scenario 5. Hypothetical event: 1938 rupture plus Shumagin gap.** To create a hypothetical event in the Alaska–Aleutian megathrust zone, we combined the rupture area of the 1938 earthquake with the Shumagin gap area, assuming that the rupture can propagate southwestward into the 1946 zone (figs. 1, 8). Jacob (1984) suggested that a major earthquake within the Shumagin gap has a high potential to occur in the next 20 years. Recently, Freymueller and Beavan (1999) have shown that there is no significant strain in this area, and the Shumagin segment alone is not capable of generating a great earthquake. However, we can assume that the distribution of moment along the length of the fault can vary, resulting in a multiple asperity rupture, with the 1938 zone as a major asperity and a smaller asperity in the 1946 zone, with the area of lower moment release between them. This mechanism was suggested for the 1964 earthquake by Christensen and Beck (1994).

(a)

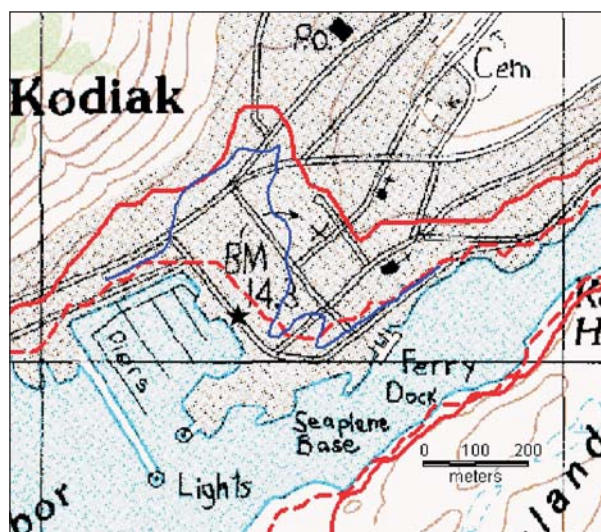


Figure 6. Observed (dark blue) and computed (red) inundation lines for the Kodiak downtown area (a) and USCGR, formerly the Kodiak Naval Station (b). Solid red line delineates inundation calculated using the 17-fault model; dashed red line represents the inundation calculated using the single-fault model. Star (a) indicates location of photograph in figure 2.

(b)

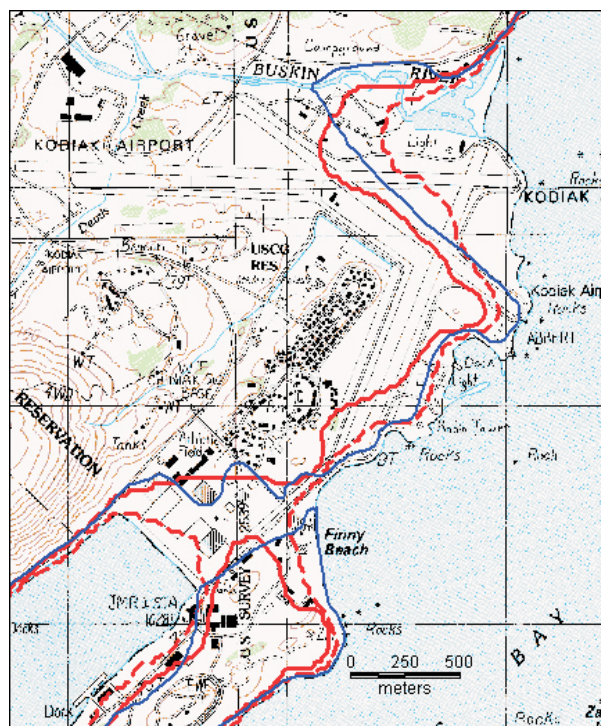


Table 3. Fault rupture parameters for single-fault scenarios

	Depth (km)	Length (km)	Width (km)	Strike (degrees)	Dip (degrees)	Rake (degrees)	Slip (m)
Scenario 2	5	800	250	221	5	90	8.2
Scenario 4	5	350	250	219.5	5	90	6.4
Scenario 5	5	800	175	245	10	90	10
Scenario 7	5	1000	80	357	12	90	10

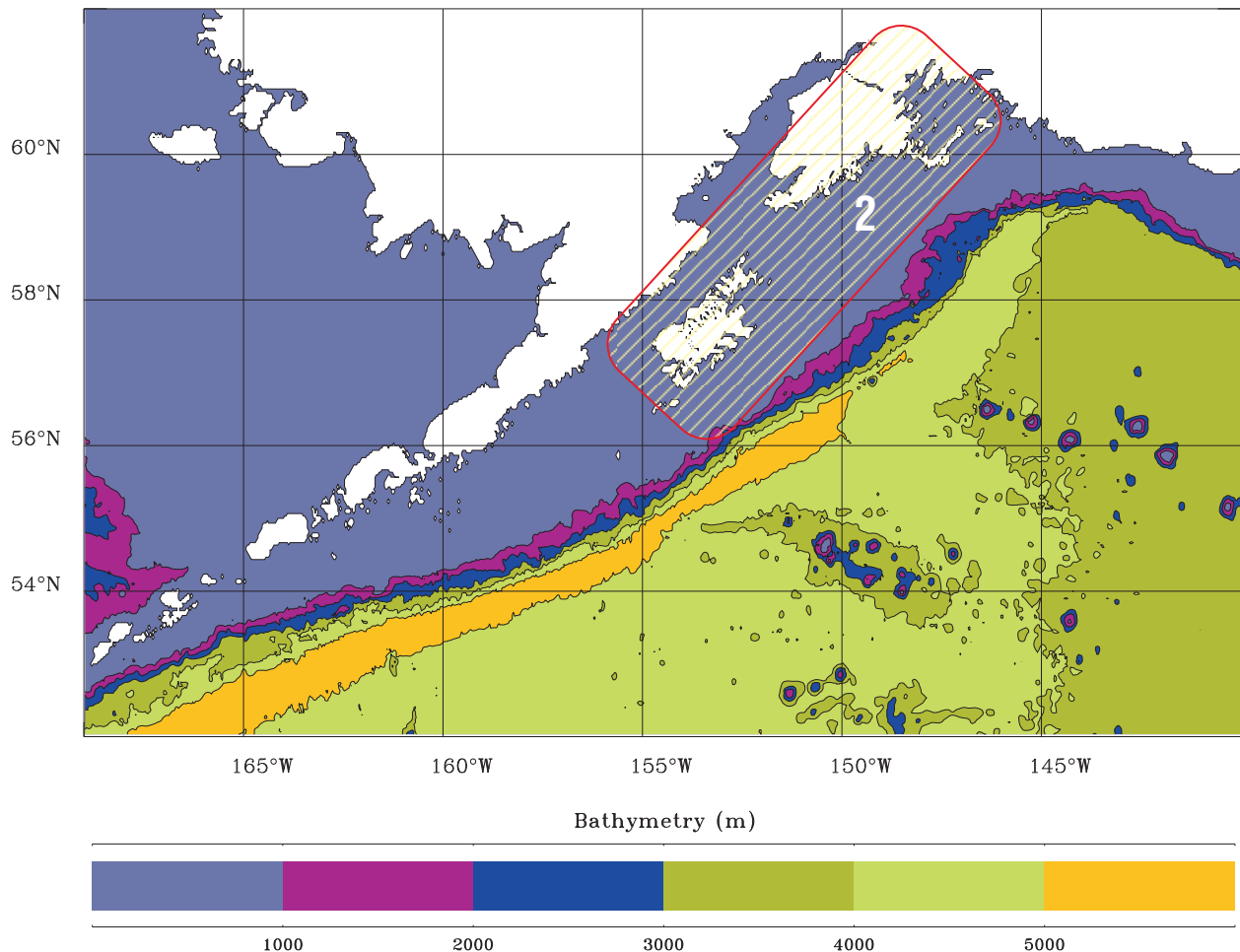


Figure 7. Rupture area of the 1964 earthquake modeled as a single fault.

**Scenario 6. Hypothetical event: Narrow Cape fault.**

The Narrow Cape fault is part of a series of northeast-trending thrust faults that extend across the southeastern Kodiak Island and into the northwestern Gulf of Alaska (fig. 9). The geomorphic expression of this fault at Narrow Cape suggests that it displaces glacial sediments deposited during the last glacial maximum. Therefore, the scarp is probably Holocene in age and worthy of consideration as a potential source for a local tsunami. We selected the 1999 ChiChi earthquake in Taiwan as a hypothetical analog for displacement on Narrow Cape fault, because the Chenlungpu fault on which that earthquake occurred is in a very similar tectonic setting. Vertical offset on the Chenlungpu fault ranged from about 3 m at one end to 10 m at the other end. We constructed three different source functions for the Narrow Cape fault scenario. The rupture area of 80 km by 35 km shown in figure 9 is divided into three subfaults, and their slip values for different models are summarized in table 4.

Model A has the uniform displacement of 6 m on all faults, Model B has the maximum slip on the northeastern subfault, and Model C has the maximum slip on the south-

western subfault. The moment magnitude for all models is 7.8, dip is 70 degrees, rake is 90 degrees and strike is 227 degrees. Our numerical experiments show that the maximum inundation results from the wave generated by the Model C earthquake. Therefore, this model was chosen to represent the Narrow Cape fault scenario on the inundation maps.

**Scenario 7. Cascadia subduction zone rupture.** This scenario represents one of the distant tsunami sources that can affect the Kodiak Island communities. Atwater and others (1995) summarized the geologic evidence for past great earthquakes at the Cascadia subduction zone. The last such event occurred about 300 years ago, and the authors estimated the recurrence interval to be about 200–600 years. The rupture area of the hypothetical Cascadia subduction zone earthquake is shown in figure 10. To propagate the wave from the source to Alaska coastlines, we added one more grid of 6-minute resolution that covers the Pacific Ocean north of the equator. This grid is connected to the 2-minute grid that covers the Gulf of Alaska.

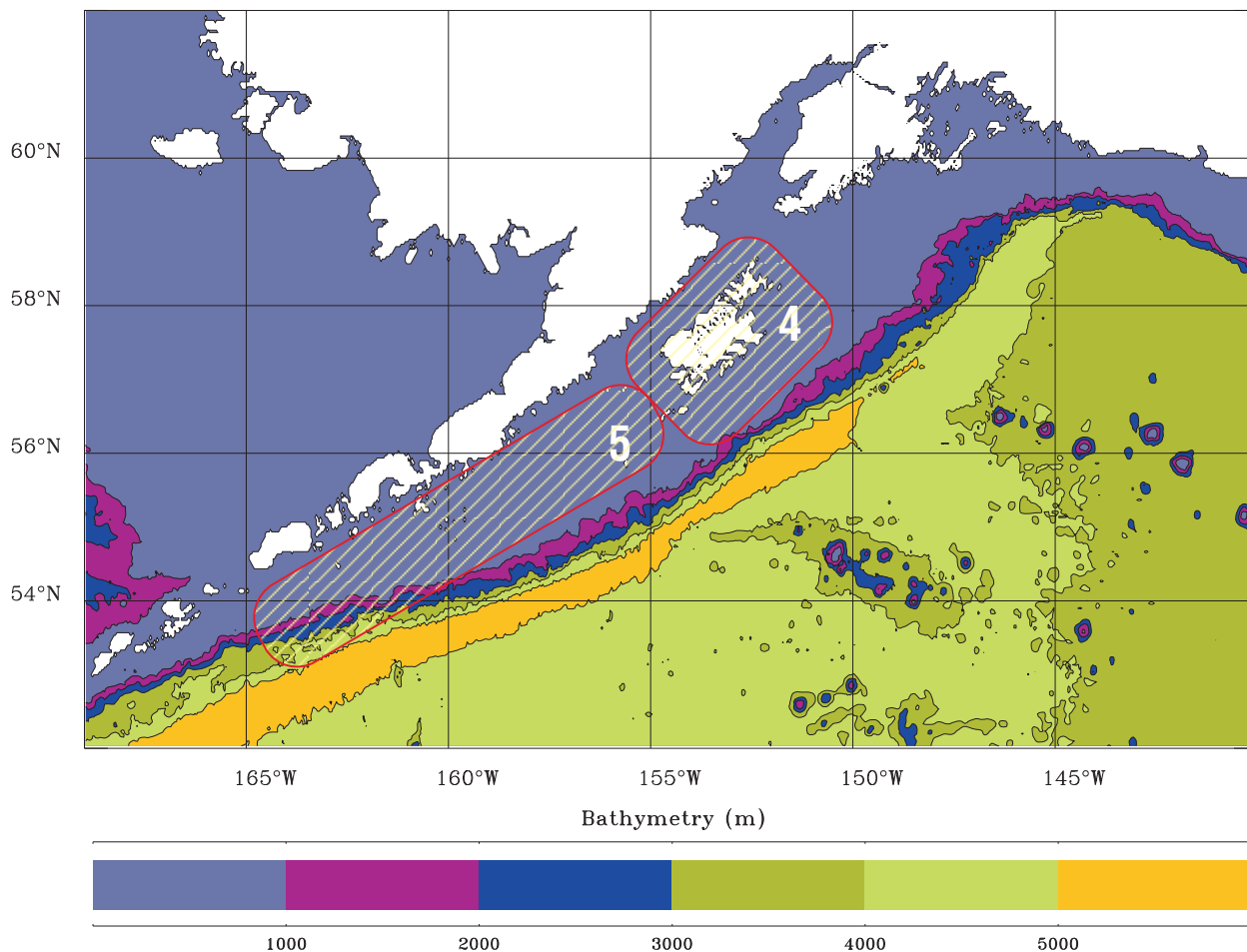


Figure 8 (above). Rupture areas of the two hypothetical earthquakes in the Alaska–Aleutian megathrust zone: the Kodiak asperity of the 1964 earthquake modeled as a single fault (scenario 4) and the hypothetical event with the rupture area that combines the Shumagin gap and the 1938 rupture (scenario 5).

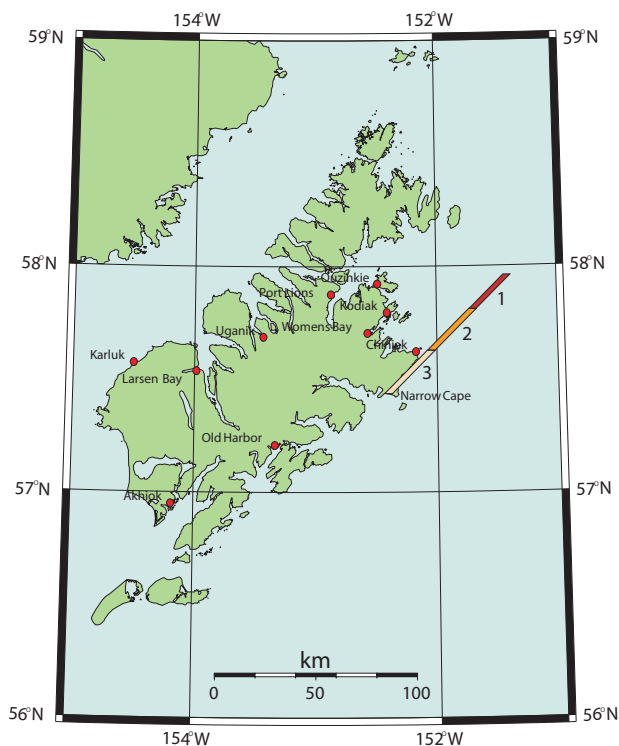


Figure 9 (left). Rupture area of Narrow Cape fault divided into three subfaults. Parameters of the subfaults are presented in table 4.

### INUNDATION MODELING RESULTS

We performed numerical calculations for all scenarios. In every case, the initial water disturbance propagated through the set of embedded grids of increasing resolution. In the three final grids of 21.8 m x 21.5 m resolution, where bathymetric and topographic data are combined in a continuous data set, we computed the extent of inundation using the moving boundary condition. The results show that with the exception of part of Womens Bay, the worst-case tsunami scenario for the three Kodiak communities is still the inundation caused by the modeled 1964 event with 17 subfaults. Comparison between the two source models for the Kodiak asperity (scenarios 3 and 4) indicates that the scenario 3 model, which takes into account the detailed slip distribution on eight subfaults, generates

greater inundation than the single fault model. Modeling results for the hypothetical tsunami originated in the 1938 rupture zone and Shumagin gap (scenario 5) suggest that it will direct its energy mostly east and southeast, producing very little inundation in Kodiak. The Narrow Cape fault source produced the second-largest inundation zone after the inundation caused by the 17-fault model of the 1964 earthquake in almost all locations, and exceeded the modeled 1964 inundation in part of Womens Bay. This result implies that the local offshore earthquake of a smaller magnitude can generate a wave comparable to that produced by the great megathrust earthquake. As for the hypothetical tsunami originated at the Cascadia subduction zone (scenario 7), a major part of the tsunami energy will be directed west and southwest, toward Hawaii, and a limited amount toward coastlines of Alaska.

Table 4. Slip distribution for the Narrow Cape scenarios

	Model A	Model B	Model C
Subfault 1 (25 km x 35 km)	6 m	9.6 m	3 m
Subfault 2 (30 km x 35 km)	6 m	6 m	4.9 m
Subfault 3 (30 km x 35 km)	6 m	3 m	9.6 m

### LOCAL OBSERVATIONS

In addition to the mapped 1964 inundation in downtown Kodiak and USCGR (Kachadoorian and Plafker, 1967), we obtained local observations to help estimate the actual inundation at other locations in our project area. These included observations by local residents who were

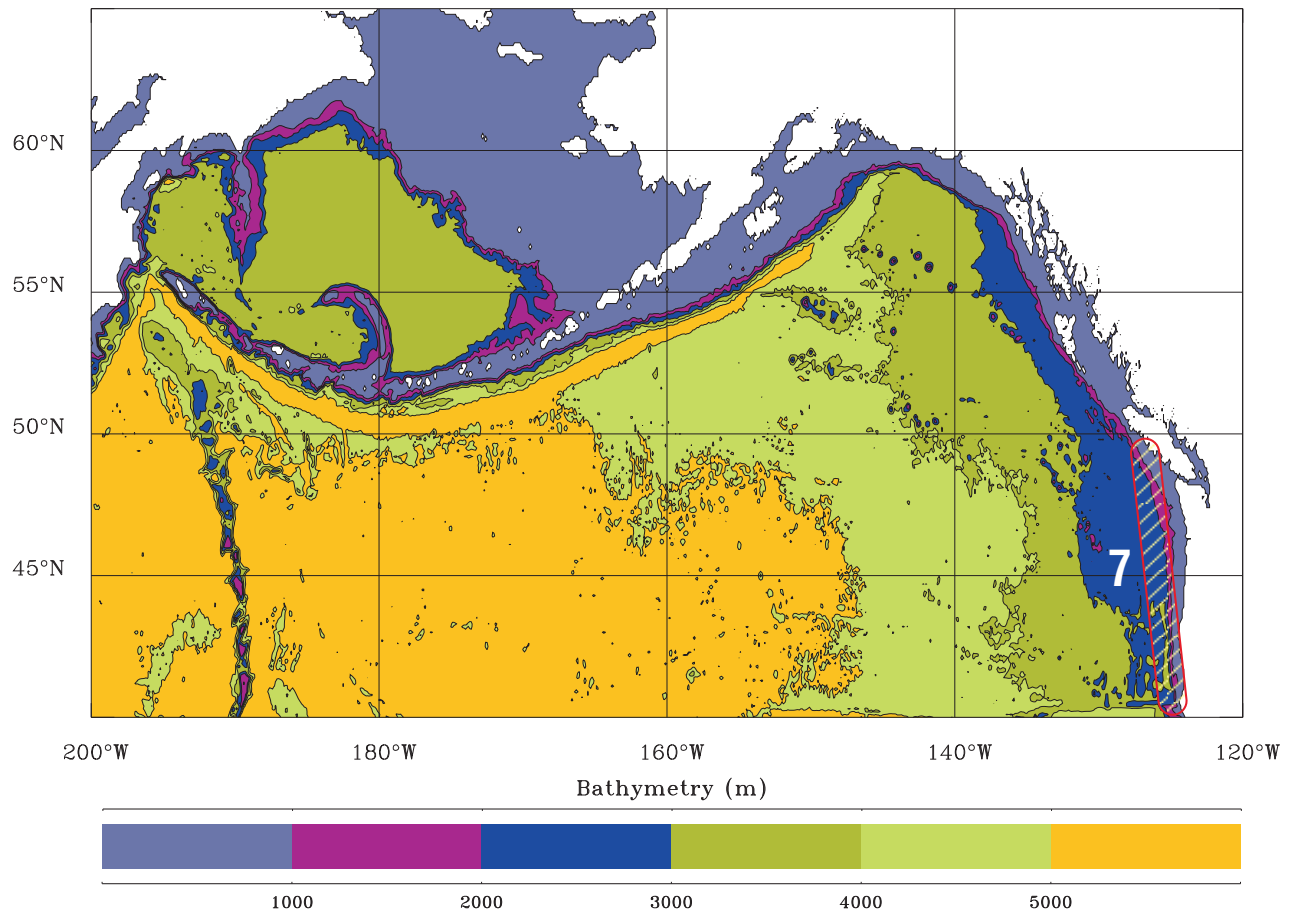


Figure 10. Hypothetical event in the Cascadia subduction zone modeled as a single fault.

present at the time of the 1964 event; the inland extent of driftwood and tsunami sand layer in the vicinity of Womens Bay; and inspection of Reuben Kachadoorian's personal notes and photographs at the Anchorage office of the U.S. Geological Survey. These observations, shown on sheets 1 and 2, identified a few areas where the actual inundation in 1964 extended farther inland than the inundation from any of our modeled scenarios, most notably in the vicinity of Womens Bay. The maximum inundation lines shown on sheets 3 and 4 include these areas of locally documented effects of the 1964 tsunami. Although the driftwood line is a reliable indicator of inundation limit, we did not attempt to estimate how much farther inland the 1964 inundation may have extended beyond the observed effects in other areas.

### **TIME HISTORIES**

In order to provide more accurate assessment of tsunami hazard for any particular community, we supplement the inundation maps with information about the time history of the wave action in the region. The time of arrival of the first wave, the wave with the maximum amplitude, and duration of the wave action are important factors that have to be considered by emergency managers during evacuation planning. We computed time histories of tsunami waves offshore of three locations (Kodiak city harbor, Shahafka Cove, and USCG Reservation) for scenarios 1, 6, and 7 that represent both local and distant sources as well as the worst-case scenario. The zero time corresponds to the epicenter origin time, and the zero water level corresponds to the post-earthquake MHHW level. Figure 11a shows change in sea level at the Kodiak city harbor (point 1 on sheet 3) for the modeled 1964 event and for the Narrow Cape fault scenario. Sea level change due to the Cascadia earthquake is shown in figure 11b. The wave arrives much sooner in the case of the local Narrow Cape fault event, because all three Kodiak communities are located in the area of coseismic uplift. The maximum amplitude wave arrives about 2 hours after the earthquake

in the case of the 1964 event. It takes the wave about 5 hours to travel to Kodiak from the Cascadia subduction zone. Figures 12 and 13 show similar results for the two other locations. We also computed velocity time histories for Near Island channel (point 3 on sheet 3), which is shown in figure 14a for scenario 1. Figure 14b shows velocity time history at the mouth of Buskin River (point 7 on sheet 4) for scenario 6. These plots demonstrate that current speed could be very high and change rapidly. Table 5 summarizes other critical parameters for nine locations indicated on sheets 3 and 4. These are maximum sea level and depth of inundation on dry land, the minimum water depth, values of maximum velocity and the direction of the maximum velocity vector.

The tsunami generated by the 1964 earthquake was recorded on a number of tide gauges around the Pacific Ocean. Many of these records are from Spaeth and Berkman (1972). Also, Lander (1996) gives marigrams from Alaska tide stations for the 1964 tsunami event. Wilson and Torum (1968) constructed the hypothetical marigrams based on eyewitness observations for several locations along the affected coastline.

### **SOURCES OF ERROR**

The source mechanism remains the biggest unknown in the problem of tsunami modeling. Since the initial condition for the modeling is determined by the displacement of the ocean bottom, the largest source of error is the earthquake model. When the tsunami is generated in the vicinity of the coast, the direction of the incoming waves, their amplitudes and times of arrival are determined by the initial displacements of the ocean surface in the source area, because the distance to the shore is too small for the waves to disperse. Therefore, the near-field inundation modeling results are especially sensitive to the fine structure of the tsunami source. It is much easier to introduce errors in the modeling process when the complexity of the source function is combined with the proximity of the coastal zone. Model runs for the 17-subfault scenario

Table 5. *Some critical parameters at 9 locations indicated on sheets 3 and 4*

Point number	Sheet number	Maximum sea level and depth of inundation on dry land, meters	Minimum water depth, meters	Maximum velocity, meters/sec	Azimuth of maximum velocity vector (from true north)
1	3	3.34	6.29	3.14	345
2	3	2.30	n/a	4.19	278
3	3	3.31	10.50	5.34	90
4	3	5.14	n/a	4.99	164
5	3	3.56	0	5.67	281
6	4	6.00	n/a	3.85	77
7	4	4.12	0.10	9.00	83
8	4	4.60	3.80	1.92	65
9	4	3.00	n/a	3.95	232

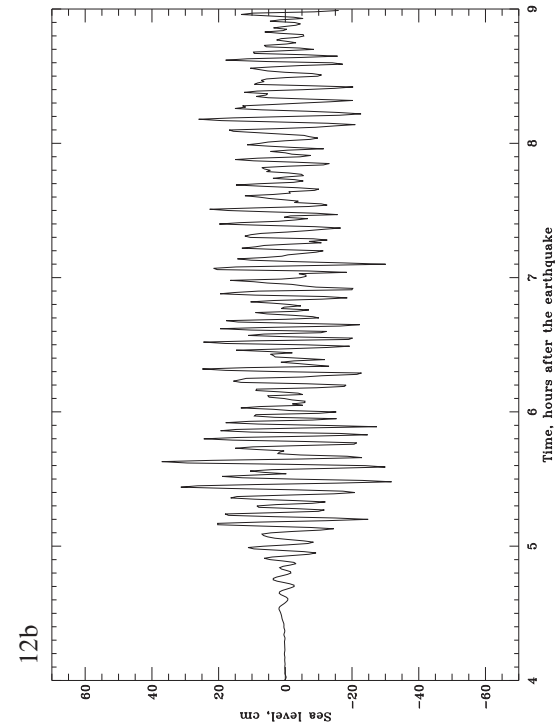
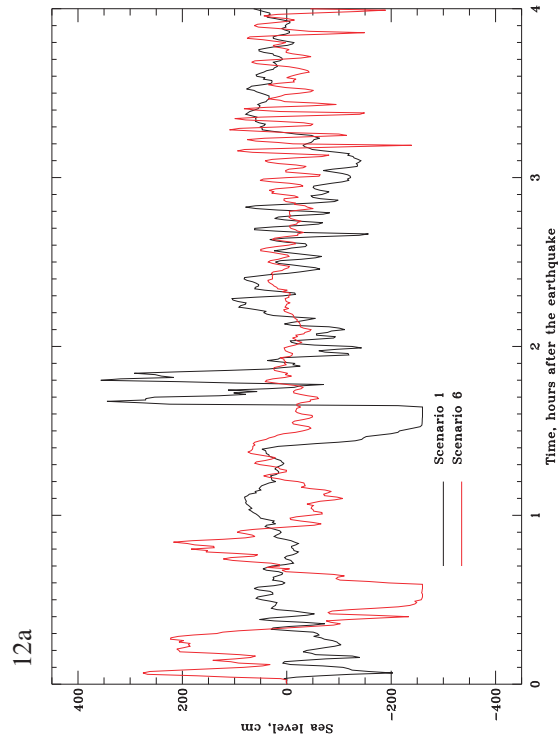
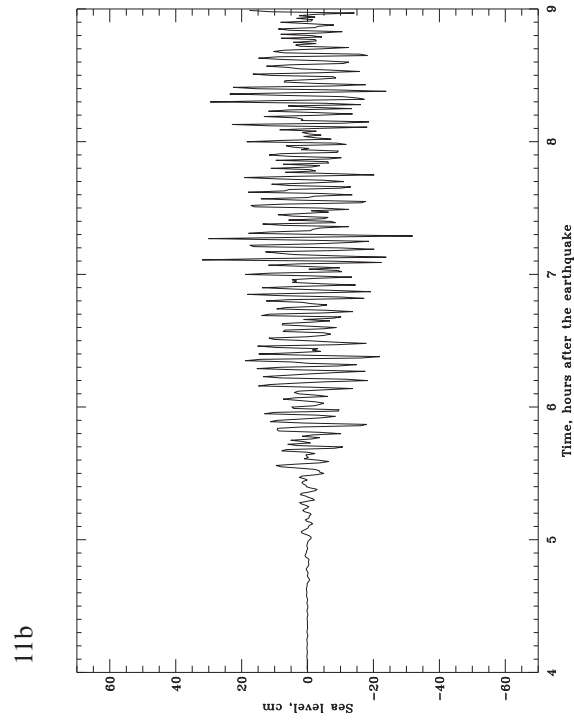
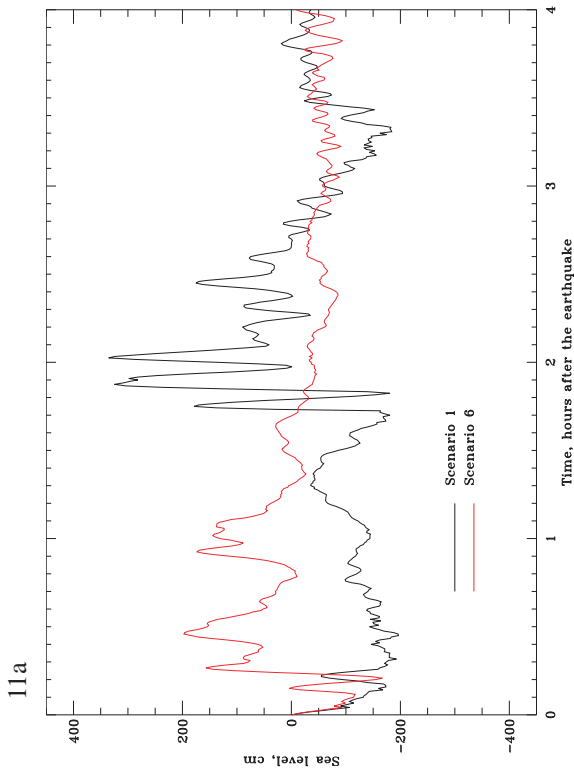


Figure 11. Time histories of modeled tsunami waves at Kodiak city harbor (point 1 on sheet 3) for scenarios 1 and 6 (a) and scenario 7 (b). 100 cm = 3.3 ft. The zero value of sea level corresponds to the post-earthquake MHHW level.

Figure 12. Time histories of the modeled tsunami waves at Shahavka Cove (point 5 on sheet 3) for scenarios 1 and 6 (a) and scenario 7 (b). 100 cm = 3.3 ft. The zero value of sea level corresponds to the post-earthquake MHHW level.

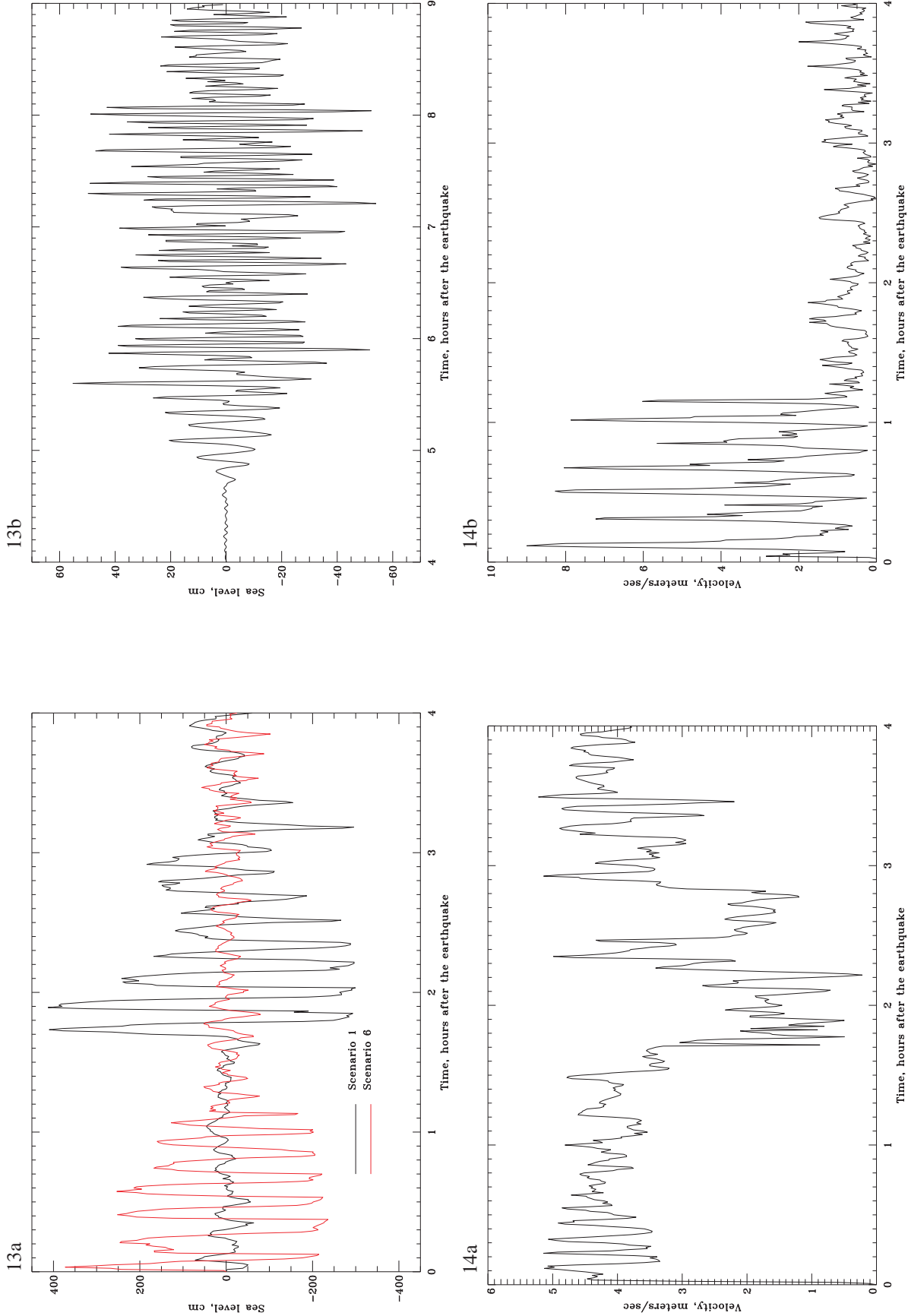


Figure 13. Time histories of the modeled tsunami waves offshore the mouth of Buskin River (point 7 on sheet 4) for scenarios 1 and 6 (a) and scenario 7 (b). 100 cm = 3.3 ft. The zero value of sea level corresponds to the post-earthquake MHHW level.

Figure 14. Velocity time histories in Near Island channel (point 3 on sheet 3) for scenario 1 (a) and at the mouth of Buskin River (point 7 on sheet 4) for scenario 6 (b). 1 m/sec = 1.94 knots.

of the 1964 earthquake have shown that modifying the amount of slip on individual subfaults can cause changes in the maximum amplitude arrivals and extent of inundation at particular locations.

Another source of error is inaccuracy of bathymetric and topographic data used in the model. Adequate bathymetric data for inundation modeling are not available for many coastal communities. For the region of Kodiak Island, bathymetric grids were constructed on the basis of data that were collected at different times and used different datums. The topographic data used in this project are non-standard 10-m DEMs that were derived by digitizing the existing USGS topographic maps, for which maximum vertical error is one-half the contour interval, or 10 m. Unfortunately, we were not able to acquire digital topographic data with higher resolution and accuracy. On the other hand, taking advantage of higher resolution topographic data would require splicing them with the bathymetric data of the same level of resolution and accuracy. That poses a limit on the quality of the combined data set, because a new bathymetric survey would be required to substantially improve the resolution of bathymetric data. Additionally, Alaska is a very dynamic region, where tectonic processes change reference levels constantly. As a result, it is extremely difficult to match bathymetric and topographic data at a shoreline for the purpose of constructing the continuous data set required for the inundation modeling.

One of the factors that affect the behavior of tsunami waves when they inundate dry land is bottom friction. The discussion of the different types of the bottom friction terms used in tsunami modeling, and their uncertainties, is given by Titov and Synolakis (1998). In this work, we use the Chesny form of the bottom drag coefficient, as it is described in Kowalik and Murty (1993b) with the value of  $r = 0.0033$ . We assumed that the reason for the mismatch in 1964 observed and calculated inundation zones in Womens Bay is bottom friction due to shallow depths in the bay. However, we conducted an experiment calculating inundation in Womens Bay without including bottom friction terms in the model, and the results differed very little.

The resolution of the grids used for inundation modeling is 21.8 m by 27.5 m, or 72 by 91 ft (at  $57^{\circ}47'$  latitude), which is limited by the resolution of the topographic and bathymetric data used for the grid construction. This resolution is high enough to describe major relief features, although there are some important structures that cannot be resolved by this grid. For example, we modeled breakwaters as artificial walls between two adjacent grid points. Obviously, buildings and other facilities also cannot be accurately resolved by the existing model. The limited resolution of the grid also affects the position of the inundation line. In order to calculate the extent

of inundation, the value of zero is assigned to all “dry” grid points, and the value of one is assigned to all “wet” points at the beginning of computation. The position of the boundary between dry and wet points changes during the process of multiple tsunami wave runups, but once a point turns “wet,” it stays wet. As a result, the position of the dry–wet boundary at the end of the computations represents the cumulative maximum extent of inundation from all waves. This partially accounts for the locally high variation in elevation of the maximum inundation line. Additionally, the distance between two neighboring dry and wet points could be as great as 90 ft, which represents the window of uncertainty for the position of the inundation line. At some locations with steep slopes, the change of elevation within this error interval could be 20 ft or more, which puts some obvious limits on the use of an inundation line for land-use planning.

The City of Kodiak provided us with the orthophotographic maps of downtown Kodiak and surrounding area. At some locations, these maps, which are not available as DEMs, have more topographic details than the USGS DEMs. In consideration of the above limitations on the accuracy of the model outputs, we used these orthophotographic maps to manually adjust the maximum inundation line on sheet 3 in some areas where digital topographic data differed substantially from the elevation contours of the orthophotographic maps. For example, the orthophotographic maps show the flat area at the southwest end of Gibson Cove extending inland much farther than it extends in the USGS DEM digital topography file. It allowed us to adjust the inundation zone in this area under the assumption that the flats would have been flooded if the model were run with corrected topography. Another similar location is the northeast end of Mission Lake, where we adjusted the inundation line to account for the lower elevations that are shown on the orthophotographic map compared to the USGS data.

## SUMMARY

We present the results of numerical modeling of tsunami waves for the city of Kodiak and vicinity from seven earthquake scenarios that provide an estimate of maximum credible tsunami inundation. These results are useful for state and local emergency managers to identify areas that should be evacuated in the event of a major tsunamigenic earthquake. Because of the uncertainties inherent in this type of modeling, these results are not intended for land-use planning. We also have not modeled the possible inundation by waves that might be generated by local submarine or subaerial landslides. A hypothetical major collapse of the seaward slope of Pillar Mountain into St. Paul Harbor, for example, would likely result in catastrophic local inundations that far surpass those indicated by the results of our models from tectonically

generated tsunamis. The potential for such local landslide-generated waves is unknown.

## ACKNOWLEDGMENTS

This project was supported in part by the National Tsunami Hazard Mitigation Program through NOAA grant NA67RJ0147, by the Alaska Department of Military and Veteran Affairs (grant RSA-0991007), and by Alaska Science and Technology Foundation (grant ASTF-971002). The authors wish to thank Dr. Fumihiko Imamura for the Fortran code of the Okada algorithm he kindly provided. We also thank Frank Gonzalez, Prof. Zygmunt Kowalik, and Howard Weston for their thoughtful reviews of the draft manuscript and maps.

Data used for the bathymetric and topographic grids are credited to the following sources:

National Oceanic and Atmospheric Administration, National Geodetic Database Centers: Hydrographic Surveys and Marine Geophysics Tracklines, GEODAS Version 3.3 and Version 4.0 Software. Boulder, Colorado. Website reference: <http://www.ngdc.noaa.gov/mgg/bathymetry/relief.html>.

U.S. Geological Survey, National Mapping Division: Topographic Digital Elevation Models. Reston, Virginia. Website reference: <http://mapping.usgs.gov/>.

U.S. Army Corps of Engineers—Alaska District: Hydrographic Surveys for Kodiak. Anchorage, Alaska. Website reference: <http://www.poa.usace.army.mil/>.

Scientific Fishery Systems, Inc.: Bathymetric Soundings Data for Alaska. Anchorage, Alaska. Website reference: <http://www.scifish.com/>.

## REFERENCES CITED

- Atwater, B.F., Nelson, A.R., Clague, J.J., Carver, G.A., Yamaguchi, D.K., Bobrowsky, P.T., Bourgeois, J., Darienzo, M.E., Grant, W.C., Hemphill-Haley, E., Kelsey, H.M., Jacoby, G.C., Nishenko, S.P., Palmer, S.P., Peterson, C.D., and Reinhart, M.A., 1995, Summary of coastal geologic evidence for past great earthquakes at the Cascadia subduction zone: *Earthquake spectra*, v. 11, no. 1, p. 1–18.
- Christensen, D.H., and Beck, S.L., 1994, The rupture process and tectonic implications of the Great 1964 Prince William Sound earthquake: *Pageoph*, v. 142, no. 1, p. 29–53.
- Freymueller, J.T., and Beavan, J., 1999, Absence of strain accumulation in the western Shumagin segment of the Alaska subduction zone: *Geophysical Research Letters*, v. 26, no. 21, p. 3233–3236.
- Jacob, K.H., 1984, Estimates of long-term probabilities for future great earthquakes in the Aleutians, *Geophysical Research Letters*, v. 11, p. 295–298.
- Johnson, J.M., Satake, K., Holdahl, S.R., and Sauber, J., 1996, The 1964 Prince William Sound earthquake: Joint inversion of tsunami waveforms and geodetic data: *Journal of Geophysical Research*, v. 101, no. B1, p. 523–532.
- Kachadoorian, R., and Plafker, G., 1967, Effects of the earthquake of March 27, 1964 on the communities of Kodiak and nearby islands: U.S. Geological Survey Professional Paper 542-F, 41 p.
- Kowalik, Z., and Murty, T.S., 1993a, Numerical simulation of two-dimensional tsunami runup: *Marine Geodesy*, v. 16, p. 87–100.
- Kowalik, Z., and Murty, T.S., 1993b, Numerical modeling of ocean dynamics: World Scientific, 481 p.
- Lander, J.F., 1996, Tsunamis affecting Alaska. 1737–1996: National Geophysical Data Center (NGDC): Key to Geophysical Research Documentation no. 31, 195 p.
- Murty, T.S., 1984, Storm Surges—Meteorological Ocean Tides: *Canadian Bulletin of Fisheries and Aquatic Sciences*, v. 212, 897 p.
- Okada, Y., 1985, Surface deformation due to shear and tensile faults in a half-space: *Bulletin of the Seismological Society of America*, v. 75, p. 1135–1154.
- Plafker, G., Carver, G.A., and Clarke, S.H. Jr., 2000, Seismotectonics of the 1964 Alaska earthquake as an analog for future tsunamigenic southern Cascadia subduction earthquakes, *in* Clague J., Atwater B., Wang K., Wang M.M., and Wong, I., eds., *Proceedings of the Geological Society of America Penrose Conference, Great Cascadia Earthquake Tricentennial: Oregon Department of Geology and Mineral Industries Special Paper 33*, p. 96–97.
- Reid, R.O., and Bodine, B.R., 1968, Numerical model for storm surges in Galveston Bay: *Journal of the Waterways and Harbors Division*, v. 94, no. WWI, p. 33–57.
- Spaeth, M.G., and Berkman, S.C., 1972, Tsunami of March 28, 1964, as recorded at tide stations and the Seismic Sea Waves Warning System, *in* *The Great Alaska Earthquake of 1964, Oceanography and coastal engineering*, National Academy of Sciences, Washington, D.C., p. 38–100.
- Titov, V.V., and Synolakis, C.E., 1998, Numerical modeling of tidal wave runup: *Journal of Waterway, Port, Coastal and Ocean Engineering*, July–August, p. 157–171.
- Troshina, E.N., 1996, Tsunami waves generated by Mt. St. Augustine volcano, Alaska: MS thesis, University of Alaska Fairbanks, 84 p.
- Wilson, B.W., and Torum, A., 1968, The tsunami of the Alaskan Earthquake, 1964: Engineering evaluation: U.S. Army Corps of Engineers, Technical memorandum No. 25, 401 p.

